Available online at www.sciencedirect.com

jmr&t Journal of Materials Research and Technology

journal homepage: www.elsevier.com/locate/jmrt

Original Article

First-principles calculations to investigate structural, elastic, electronic, lattice dynamic and optical properties for scandium and yttrium nitrides in zinc blend structure

Mohamed Amine Ghebouli [a,b,*], *Brahim Ghebouli* [c], *Aldjia Zeghad* [a], *Tayeb Chihi* [b], *Messaoud Fatmi* [b], *Sameh Ibrahim Ahmed* [d]

[a] *Department of Chemistry, Faculty of Technology, University of Mohamed Boudiaf, M'sila, 28000, Algeria*
[b] *Research Unit on Emerging Materials (RUEM), University Ferhat Abbas of Setif 1, Setif, 19000, Algeria*
[c] *Laboratory of Studies Surfaces and Interfaces of Solids Materials, Department of Physics, Faculty of Science, University Ferhat Abbas of Setif 1, Setif, 19000, Algeria*
[d] *Department of Physics, College of Science, Taif University, P.O. Box 11099, Taif, 21944, Saudi Arabia*

ARTICLE INFO

Article history:
Received 27 April 2021
Accepted 15 July 2021
Available online 21 July 2021

Keywords:
Castep
Zinc blend
Nitride
Band structure
Band gap
Absorption

ABSTRACT

We studied the structural, elastic, electronic, dynamic and optical properties of scandium and yttrium nitrides in the zinc blend structure. The GGA, LDA and GGA-PBESOL approaches, as well as the HSE hybrid functional, were used in the representation of the electronic exchange and correlation effects. The lattice constant, the bulk modulus and its pressure derivative calculated in the HSE hybrid approach are predictions. The elastic constants and B/G ratio infer that ScN and YN are elastically stable and ductile in nature. ScN and YN in the zinc blend structure show an isotropic linear compressibility and anisotropic Young's modulus, shear modulus and Poisson's ratio. The anisotropy and hardness in ScN and YN compounds are more pronounced in the LDA approach. The X–X (W–W) direct band gap in scandium (yttrium) nitride translates its semiconductor character in the zinc blend structure. The N: p orbit and small contribution of Sc: d (Y: d) site are responsible to the optical modes, while Sc: d (Y: d) site and small contribution of N: p orbit are the sign of acoustical modes. The absorption peaks are assigned to photo transitions energies from maximum valence band to minimum conduction band.

* Corresponding author.
E-mail address: med.amineghebouli@yahoo.fr (M.A. Ghebouli).

https://doi.org/10.1016/j.jmrt.2021.07.073

1. Introduction

The chemical inorganic scandium and yttrium nitride are composed of Sc (Y) as cation and N anion. Yttrium nitride is a rare type of nitride; it remains stable at high temperature and applies to refractory materials. The interest in the study of ScN lies in the fact that its field of application is quite broad such as a potential thermoelectric energy conversion device because of its lower resistivity. Various approximations such as GGA, LDA, GGA-PBESOL and HSE hybrid have been applied in this work to obtain adequate structural, elastic, electronic, dynamical and optical properties in scandium and yttrium nitrides in the zinc blend structure. The absorption spectrum shows that ScN and YN of the zinc blend structure have a low absorption in the visible light region 37,014 cm^{-1} and 47,885 cm^{-1} together with less reflectivity 29% and 28%, and therefore this reflects their transparency nature. The direct band gap X–X (W–W) calculated for ScN (YN) with GGA, LDA, GGA-PBESOL and HSE hybrid 2.40 eV, 2.28 eV, 2.34 eV and 3.28 eV (2.01 eV, 2.10 eV, 2.14 eV and 2.74 eV) translates their semiconductor character. The absorption and reflectivity of ScN (YN) in ultra violet light region are 240,000 cm^{-1} (236,000 cm^{-1}) and 45% (57%). The elastic constants, band gaps and optical transitions for ScN and YN in the zinc blend structure are computed for the first time. We explain the origin of dielectric function peaks as optical transitions from upper three valence bands to lower seven conduction bands. In our study of phonons, it was found that longitudinal and transversal optical branches are separated by a frequency gap 62.4 cm^{-1} (67.9 cm^{-1}) in ScN (YN). Also, there is a frequency gap 73.44 cm^{-1} (127 cm^{-1}) between optical and acoustical modes in ScN (YN). The hybridization between Sc: d (Y: d) and N: p in the upper valence band translates the covalent character of the link Sc: d - N: p (Y: d - N: p) [1]. For works carried out by other researchers, it is noted that scandium nitride shows some physical and mechanical parameters such as high hardness and melting point identical to those of AlN [2,3]. The scandium nitride shows adequate electrical, optical and chemical characteristics, which make it technologically interesting as ohmic contact and candidate for thermoelectricity in high temperature due to its high thermoelectric power factor [3,4]. An experimental electronic characterization of ScN thin film realized by technical optic and technical optic combined with scanning tunneling spectroscopy has a minimum gap of 1.3 ± 0.3 eV and 0.9 ± 0.1 eV [5]. Another experimental structural and electronic study indicates that scandium nitride has the lattice constant 4.501 Å and an indirect band gap Γ-X located between 0.9 eV and 1.6 eV [6–8]. A theoretical study of scandium nitride was carried out in the rocksalt phase [9–11]. The study conducted by Noboru Takeuchi reports that scandium and yttrium nitrides crystallize in the rocksalt structure and transform into CsSl phase at high pressure [9]. The high value of hardness and melting point make ScN and YN as possible potential for applications in magnetic recording and sensing, as well as refractory electronics and plasmonics materials [12,13]. Sc and Y based nitrides show features such as high mechanical strength, adjustable energy gap, transparency nature and lower reflectivity that make them as potential in optoelectronics [14]. The study realized by Joris More-Chevalier et al. reports that scandium and yttrium nitrides are characterized by high electron mobility [15]. The investigation of electronic properties for ScN and YN in the rocksalt structure indicates that these compounds have great potential for applications in photovoltaic and photo catalysis [16]. Debdeep Jena et al. identified that the family Sc and Y based nitrides are highly piezoelectric because of their high piezoelectric coupling coefficient and potentially ferroelectric materials [17]. The purpose of this work is that scandium and yttrium nitrides interest the researchers as absorbent materials, due to their high optical absorption, low reflectivity, low cost, tunable band gap and high conversion efficiency for photovoltaic applications.

The paper is organized as follows: The detail of computational method is provided in the second part. The computed results are presented and discussed in the third part. The paper is closed with brief conclusion in the last part.

2. Calculations details

The calculations were performed using the pseudo-potential plane-wave method as implemented in the CASTEP code [18]. The interaction between valence electrons and ions cores is represented by Vanderbilt ultra soft pseudo-potential [19]. The exchange-correlation effect is described in the LDA framework of Teter and Pade [20], GGA and GGA-PBESOL of Perdew et al. [21] and HSE hybrid functional. The cut off energy (E_{cut} of 660 eV), with a real space sampling grid and k-points of 8 × 8 × 8 [22], within the Monkhorst–Pack scheme [23] ensure well convergence of computed structure and energy. We optimized the lattice constant at a fixed volume of the unit cell which corresponds to the minimum energy. The summing was carried out on the Brillouin area to ensure well convergence of computed structures and energies. The calculation of the optical quantities requires the use of dense mesh of uniformly distributed 20 × 20 × 20 k-points. The structural parameters were determined by the minimization technique of BFGS [24], which provides a fast way to find the lowest energy structure. In addition, all the lower states in the calculations were treated as core states [25]. The tolerance for

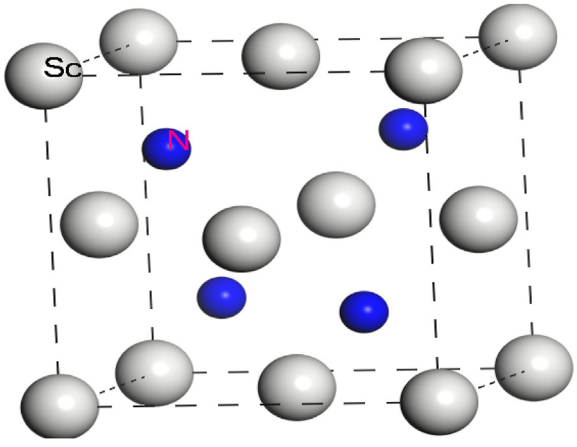

Fig. 1 – The zinc blend structure of scandium nitride.

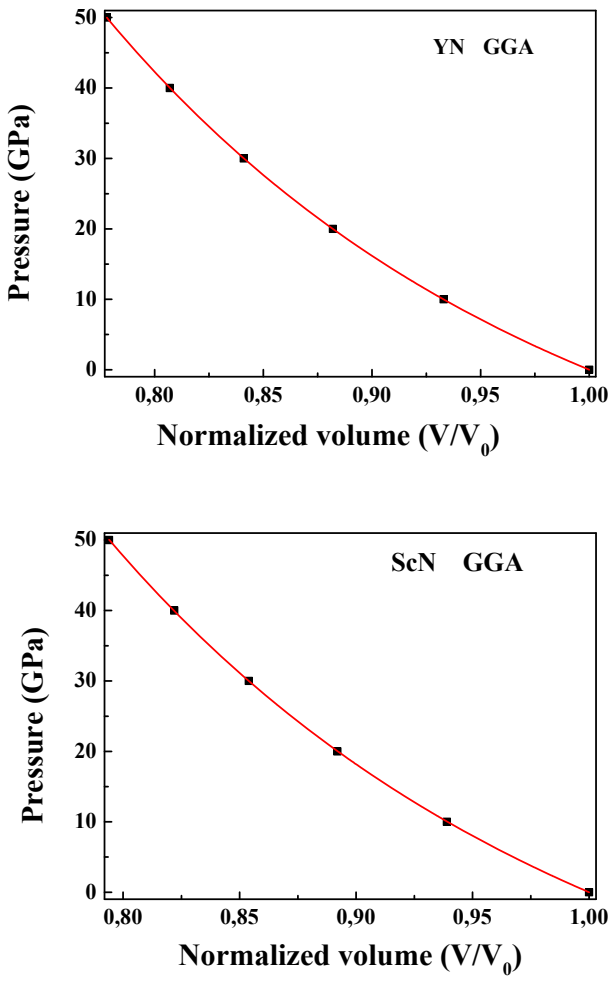

Fig. 2 – Effect of pressure on normalized volume for ScN and YN in the zinc blend structure.

geometry optimization was set as difference of total energy 5×10^{-6} eV/atom, maximum ionic Hellmann–Feynman force 10^{-2} eV/Å and maximum stress 2×10^{-2} V/Å^3.

3. Results and discussions

3.1. Crystal structure

The electronic configuration of Sc, Y and N atoms is Sc: [Ar] $4s^2$ 3 d^1, Y: [Kr] $5s^2$ 4 d^1 and N: [He] $2s^2$ $2p^3$. The scandium and yttrium nitrides crystallize in the zinc blend cubic structure. Fig. 1 shows the zinc blend structure of ScN. The atomic positions are Sc (Y): (0, 0, 0) and N: (1/4, 1/4, 1/4). The structural parameters were computed in the ground state from ab-initio computation of P (V/V_0) data. Fig. 2 presents the effect of pressure on unit cell volume ratio in the zinc blend structure for ScN and YN semiconducting. We report in Table 1 the equilibrium structural parameters for scandium and yttrium nitrides calculated within LDA, GGA and HSE hybrid functional in the zinc blend structure. These parameters computed within HSE functional are predictions. The lattice constant of scandium and yttrium nitride determined by GGA and LDA approximation are closer to those given by other calculations [26–30]. It is noted that GGA, LDA and HSE hybrid functional overestimate the lattice constant with respect to the experimental value [31,32]. The results of B_0 and B' for ScN and YN calculated within GGA and LDA using the fitting scheme P (V/V_0) agree reasonably with experimental data [31,33] and other calculations [10,29,30,34,35]. The difference between our results and those cited in the literature may be attributed to the use of various exchange–correlation functional and potentials.

3.2. Elastic constants and mechanical parameters

In ab-initio computation, there are two methods of calculating elastic constants, the volume conservation technique and the stress stain [36]. The elastic constants provide information on binding between adjacent atomic planes, the anisotropic character of bonds and elastic stability. Scandium and yttrium nitrides are studied in the zinc blend structure, therefore, three independent constants C_{11}, C_{12} and C_{44} require for their elastic characterization. The elastic moduli at equilibrium for scandium and yttrium nitrides computed using GGA, LDA and GGA-PBESOL functional are summarized in Table 2. There are no experimental and theoretical data for elastic constants of ScN and YN to be compared with our results. Consequently, future experimental measurements will test our prediction computation. The bulk modulus is inversely proportional to the volume of the unit cell. The bulk modulus is given according to elastic constants C_{11} and C_{12} by $B = (C_{11} + 2C_{12})/3$ [37,38]. Therefore, these elastic constants depend on the lattice constant. The key criterion for mechanical stability of a crystal is that the strain energy must be positive [39]. The elastic stability of the zinc blend structure is ensured by checking the following relationship [40–43]:

Table 1 – Lattice constant, bulk modulus and its pressure derivative for ScN and YN computed within GGA-PBE, LDA and HSE hybrid functional.

	ScN				YN			
	GGA	LDA	HSE hybrid	Exp	GGA	LDA	HSE hybrid	Exp
a (Å)	4.8875 4.892 [26] 4.88 [28]	4.8001 4.761 [29]	4.911	4.50 [31]	5.4898 5.20 [27]	5.1843 5.248 [30]	5.237	4.877 [32]
B_0	142.06 215.86 [34]	159.42 171.23 [30]	142.68		119.65 146.55 [34]	126.95 116.51 [30]	141.55	
B'	3.6946 3.65 [34]	3.7087 3.634 [29]	3.942		4.6843 4.77 [10]	3.6217 4.39 [35]	4.313	

Table 2 – Elastic constants, bulk modulus B, shear modulus G, Young's modulus E_H, Poisson's ratio σ_H, anisotropy factor A^U and B_H/G_H ratio for ScN and YN in zinc blend structure.

		ScN			YN		
		GGA	LDA	GGA PBESOL	GGA	LDA	GGA PBESOL
C_{11} (GPa)		171.61	187.59	173.42	140.81	145.77	136.74
C_{12} (GPa)		124.34	143.15	129.69	108.94	115.98	106.40
C_{44} (GPa)		70.82	72.22	74.7	48.61	54.21	56.32
B (GPa)	B_V	140.1	157.96	144.26	119.56	125.91	116.51
	B_R	140.1	157.96	144.26	119.56	125.91	116.51
	B_H	140.1	157.96	144.26	119.56	125.91	116.51
G (GPa)	G_V	51.94	52.22	53.56	35.54	38.48	39.86
	G_R	39.37	38.00	37.98	26.70	125.91	27.01
	G_H	45.66	45.11	45.77	31.12	125.91	33.43
E_H (GPa)		123.56	123.58	124.19	85.92	89.59	91.55
σ_H		0.35	0.37	0.36	0.38	0.38	0.37
A^U		1.59	1.87	2.05	1.65	2.29	2.37
B_H/G_H		3.06	3.50		3.84	3.74	

$$0\langle C_{11}+2C_{12},\ 0\langle C_{44},\ 0\langle C_{11}-C_{12},\ C_{12}\langle B\langle C_{11} \quad (1)$$

We note that our elastic constants verify the stability criteria listed above, therefore, ScN and YN are elastically stable at ambient temperature and equilibrium pressure. Fig. 3 visualizes the dependence of elastic moduli on pressure for scandium and yttrium nitrides. It was noted that all elastic moduli computed within GGA and LDA increase monotonously when the pressure is enhanced, except C_{44} which decreases. The bulk modulus calculated from elastic constants is practically the same as obtained from equation of state fitting P (V/V_0). This is a sign of the exact calculation of our results. The scandium and yttrium nitrides have greater elastic moduli, which explain their high hardness. Pressure is an important thermodynamic parameter in everyday life. Pressure measurement is a non destructive test of metallurgical materials; and depends on the strength of the anvil material. The diamond has the highest Bulk Modulus ~440 GPa; among all known materials, so it is used as an anvil to achieve a very high pressure. The elastic constants make it possible to determine some physical and mechanical parameters such as bulk modulus, shear modulus, Young's modulus, Poisson's ratio, anisotropy factor and B_H/G_H ratio. These parameters are calculated using GGA, LDA and GGA-PBESOL and listed in Table 2. These parameters are calculated using Voigt [44], Reuss [45] and Hill [46] approximations. The typical σ value of ionic materials is 0.25 [47–49]. The Poisson's ratio of ScN and YN are greater than the limit value 0.25, and then these materials have dominantly covalent bonding character. The computed value of the factor anisotropy and B_H/G_H ratio indicate that ScN and YN show a strong anisotropy and are ductile in nature. We use ELATE software to visualize these parameters in 3D directions [50]. Fig. 4 presents the dependence on direction of Poisson's ratio, shear modulus and Young's modulus for ScN and YN. The minimum and maximum of each parameter are visualized by green and blue colors. The shape of isotropic material is spherical and any distortion from this form indicates the anisotropy. Young's modulus, shear modulus and Poisson's ratio are anisotropic. Furthermore, the predicted maximum and minimum values of Young's modulus, linear compressibility, shear modulus and Poisson's ratio for scandium and yttrium nitrides computed using GGA, LDA and GGA-PBESOL are listed in Table 3. These values prove the isotropic linear compressibility and

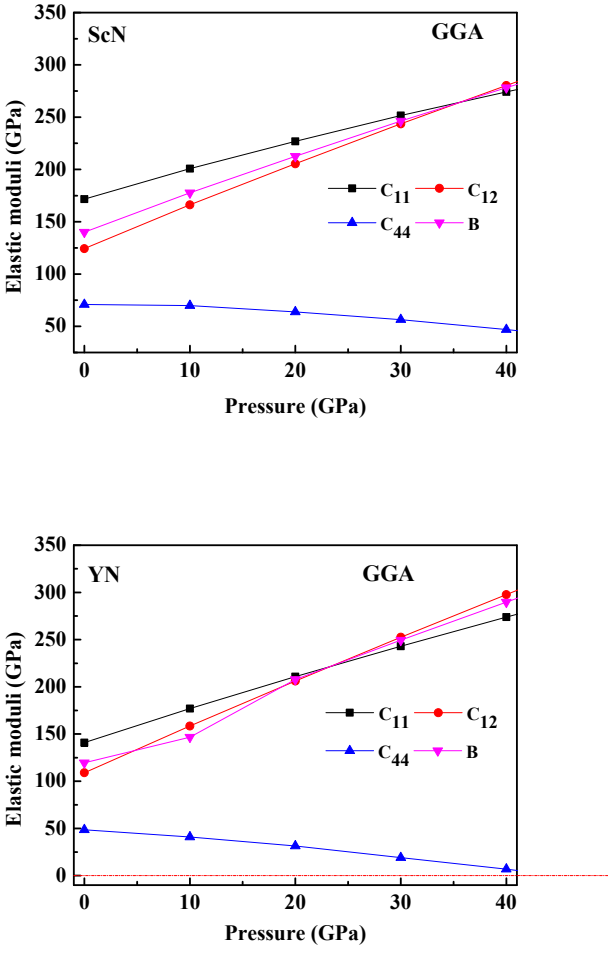

Fig. 3 – The elastic moduli as a function of pressure for ScN and YN in the zinc blend structure.

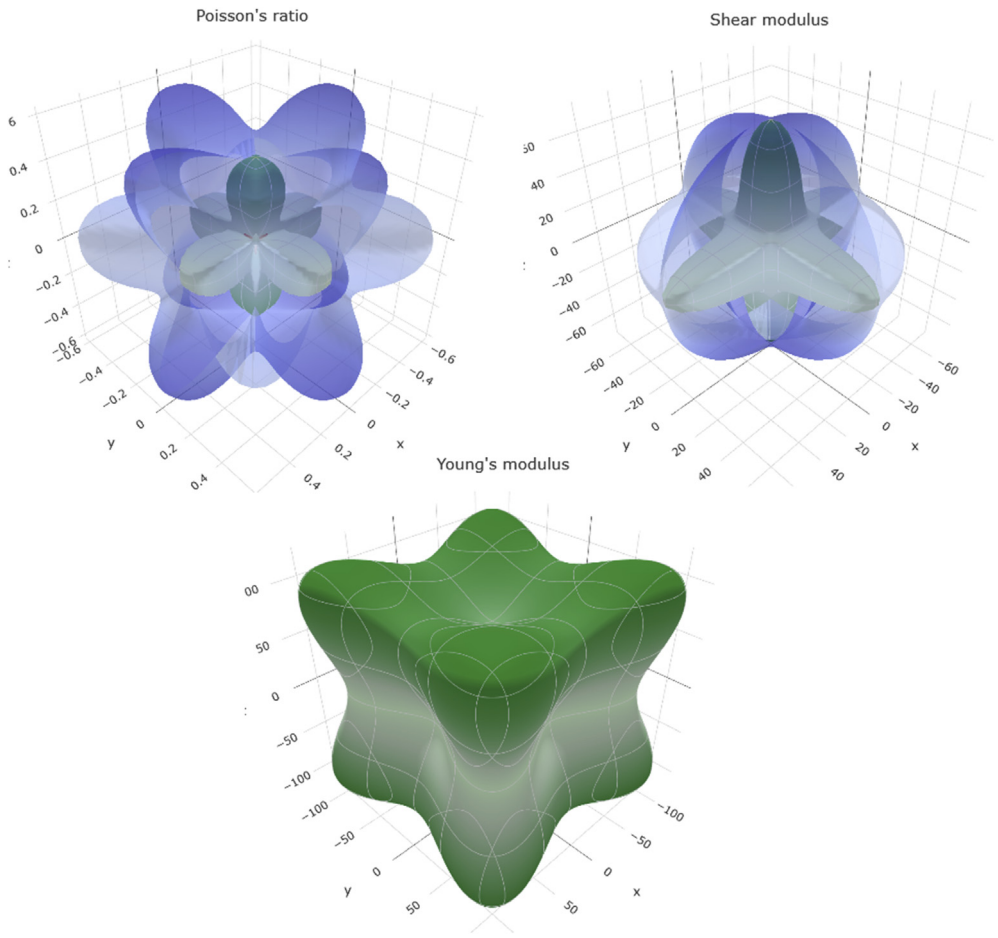

Fig. 4 – The directional dependent on Poisson's ratio, shear modulus. and Young's modulus for ScN and YN in the zinc blend structure.

confirm the anisotropy of the other parameters. From Table 3, we see also that anisotropy and hardness are more pronounced in the LDA approach.

3.3. *Electronic band structure and densities of states*

The electronic band structures for the studied scandium and yttrium nitrides were calculated using the lattice constant at equilibrium state [51] at high symmetry points W, L, Γ, X and K. The Fermi level is chosen at 0 eV and coincides with the top of the valence band. Fig. 5 shows the band structures of ScN and YN computed using GGA and HSE hybrid functional in the zinc blend phase. The bands profile indicates that ScN (YN) has a direct X–X (W–W) band gap of 2.4 eV, 2.28 eV, 2.34 eV and 3.28 eV (2.01 eV, 2.10 eV, 2.14 eV and 2.74 eV) for GGA, LDA, GGA-PBESOL and HSE hybrid functional. There are no experimental and theoretical data for band gaps of ScN and YN in the zinc blend structure, and then our results are predictions. It should be noted that LDA and GGA approximations for the exchange correlation usually underestimate the energy band gap calculated within DFT formalism [52,53]. The valence band of ScN and YN consists of two zones separated by an energy gap 8.36 eV (10.76 eV) and 8.94 eV (11.03 eV) calculated within GGA (HSE hybrid functional). The predicted direct and

Table 3 – Directional dependent on Young's modulus E, linear compressibility β, shear modulus G and Poisson's ratio σ for ScN and YN in zinc blend structure.

Parameters		Young's modulus		Linear compressibility		Shear modulus		Poisson's ratio	
		E_{min}	E_{max}	β_{min}	β_{max}	G_{min}	G_{max}	σ_{min}	σ_{max}
ScN	GGA	67.13	181.82	2.03793	2.3793	23.635	70.82	0.10051	0.79737
	LDA	63.67	188.01	2.1102	2.1102	22.22	72.22	0.12534	0.85875
	GGA_PBESOL	62.44	191.11	2.3106	2.3106	21.86	74.7	0.15573	0.86429
YN	GGA	45.776	128.45	2.7878	2.7878	15.936	48.619	0.08994	0.84324
	LDA	42.987	142.23	2.6473	2.6473	14.894	54.213	0.16829	0.92955
	GGA_PBESOL	43.62	145.52	2.8608	2.8608	15.17	56.32	0.1844	0.9216

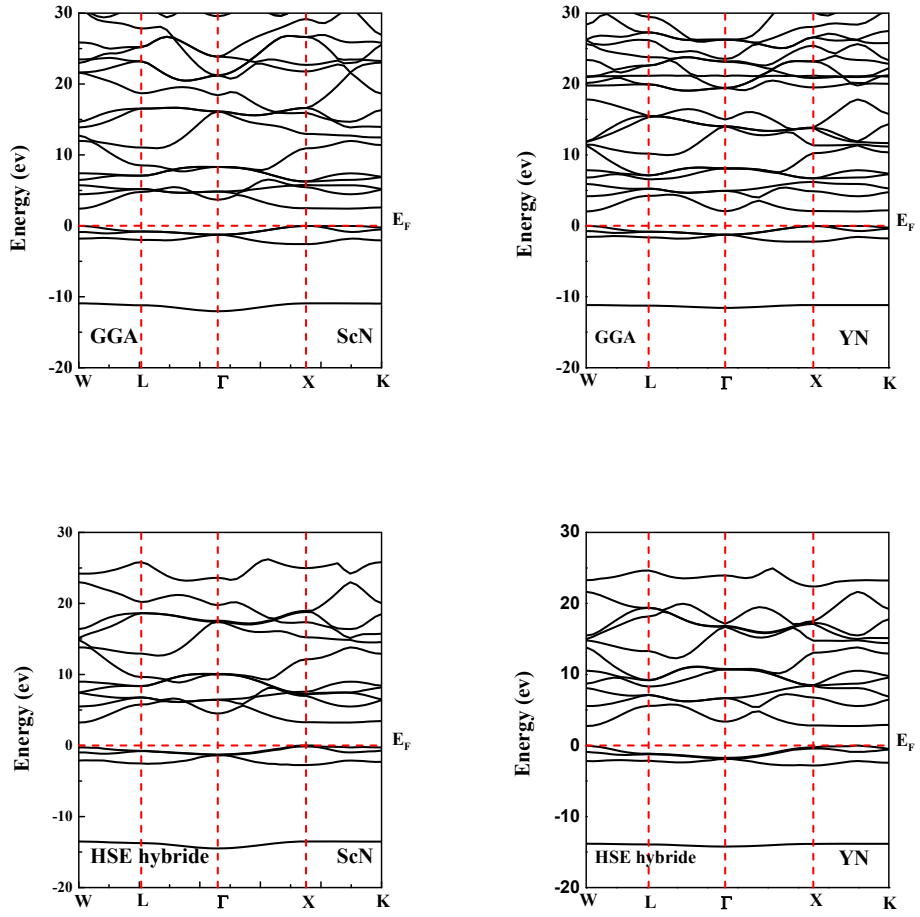

Fig. 5 – Band structures at various symmetry points into Brillouin. zone for ScN and YN in the zinc blend phase.

indirect energy band gaps at equilibrium lattice constant for binary compounds ScN and YN calculated using GGA, LDA, GGA-PBESOL and HSE hybrid are reported in Table 4. The nature of electronic states allows us to understand the role of electrons [54,55]. The plots of partial and total densities of states PDOS and TDOS were visualized in Fig. 6 for scandium and yttrium nitrides at equilibrium lattice constant. The lower valence band is located between −11.96 and −10.45 eV (−11.98 to −10.62 eV) and the upper valence band position is −2.72 eV to E_F (−2.53 eV to E_F) for ScN (YN). The valence band consists of two zones separated by a gap of 7.92 eV (8.09 eV) for ScN (YN). The electronic contribution at the top of the valence band is provided by N: p and Y: d (N: p and Sc: d) orbits, with small participation of Y: s and Y: p (Sc: s and Sc: p) sites for YN (ScN). The first conduction band of ScN (YN) starts at 2.23 eV (1.88 eV) and consisting of Sc: d (Y: d) orbit, with small contribution of Sc: s (Y: s) and N: p sites. The Hybridization between Sc: d (Y: d) and N: p in the upper valence band translates their covalent bonding character. The optical transition occurs from Sc: d (Y: d) or N: p state to Sc: p (Y: p) site.

3.4. *Phonons frequencies*

The term "phonon" means a quasi-particle associated with a progressive elastic wave. The vibrations are treated in terms of norm-modes for optical or acoustical phonons frequencies and

Table 4 – Band gaps for ScN and YN at equilibrium between various symmetry points in zinc blend structure.

Parameters		E_{L-L}	$E_{\Gamma-\Gamma}$	E_{X-X}	E_{W-W}	E_{L-X}
YN	GGA	4.99	3.35	2.08	2.01	4.24
	LDA	5.52	3.71	2.23	2.10	4.34
	HSE	6.73	5.10	3.08	2.74	5.84
	GGA_PBESOL	4.45	3.66	2.24	2.14	4.33
ScN	GGA	5.49	4.92	2.40	2.50	4.72
	LDA	5.76	4.22	2.28	2.36	4.85
	HSE	6.50	5.80	3.28	3.55	5.76
	GGA_PBESOL	5.3	5.01	2.34	2.27	3.04

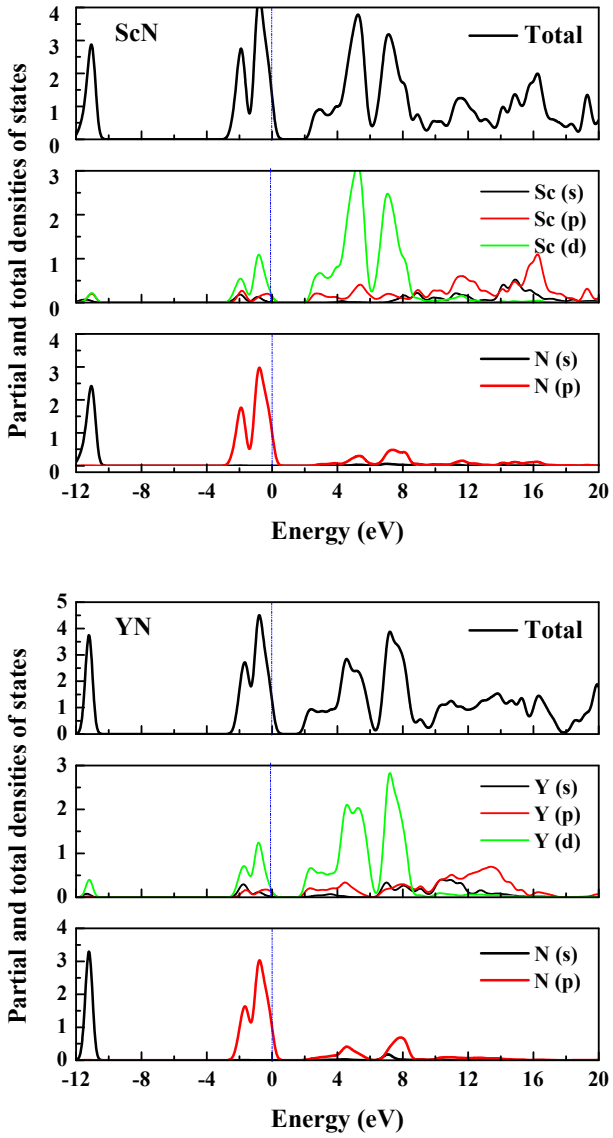

Fig. 6 – Partial and total densities of states (PDOS) and (TDOS) for ScN and YN in the zinc blend structure.

longitudinal or transversal propagation. We computed phonons dispersion curves by the density functional perturbation theory. The phonons dispersion curves and states densities of phonons for ScN and YN are visualized in Fig. 7. The longitudinal and transversal optical phonons frequencies ω_{L0} and ω_{T0} at Γ, X and L points for ScN and YN are listed in Table 5. All ScN phonons frequencies ω_{L0} and ω_{T0} are greater than those of YN. There are no soft modes and consequently these semiconducting materials are dynamically stable. We point out that the main features of phonons dispersion spectra are the followings:

1 The longitudinal optical and transversal optical branches are separated by a frequency gap 50.8 cm^{-1} (66.2 cm^{-1}) in ScN (YN).
2 There is a frequency gap 73.4 cm^{-1} (127 cm^{-1}) between optical and acoustical modes in ScN (YN).
3 The N: p orbit sand small contribution of Sc: d (Y: d) site are responsible to the optical modes.
4 The Sc: d (Y: d) site and small contribution of N: p orbit are the sign to the acoustical modes.
5 The maximum of longitudinal (acoustical) branches is located between L and Γ (at L and X) points.
6 There is overlapping between longitudinal and transversal acoustical branches.

3.5. *Optical properties*

The imaginary part of the dielectric function and transitions energies from upper three valence bands to lower seven conduction bands $E(k) = E_{Cj}(k) - E_{Vi}(k)$ are displayed in Fig. 8 (right and left panel); where V_i and C_j are the valence band

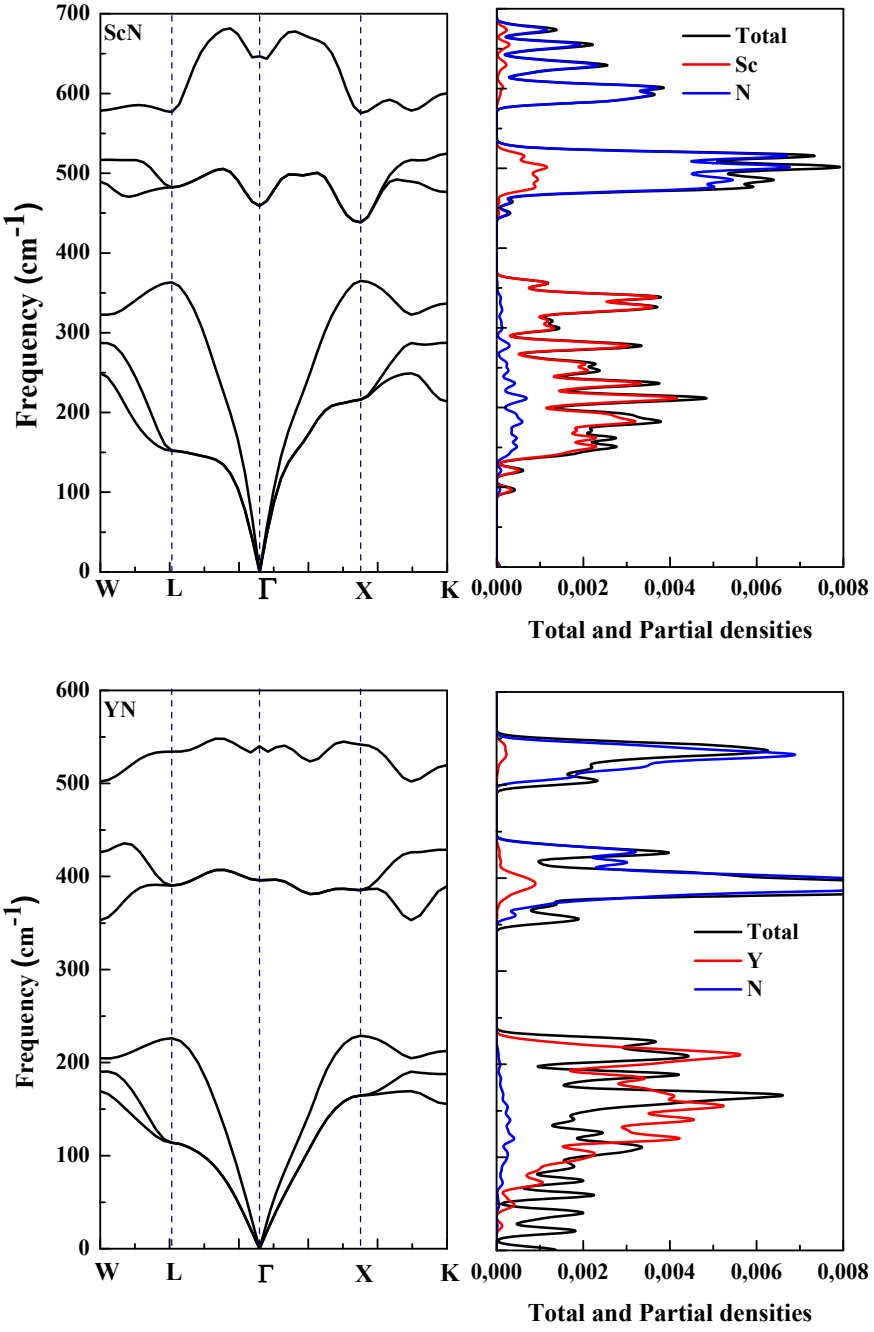

Fig. 7 – Phonons dispersion curves and states densities for ScN and YN in the zinc blend structure.

Table 5 – Longitudinal and transversal optical phonons frequencies ω_{LO} and ω_{TO} at Γ, X and L points for ScN and YN.

	Γ		X				L			
	ω_{LO}	ω_{TO}	ω_{LO}	ω_{TO}	ω_{LA}	ω_{TA}	ω_{LO}	ω_{TO}	ω_{LA}	ω_{TA}
ScN	459	647	216	361	439	575	152	363	482	577
YN	396	540	165	229	385	542	114	226	390	534

number *i* and the conduction band number *j*. The main contribution to the optical spectra originates from these possible transitions between various symmetry points in the Brillouin zone and their corresponding maximum energy are reported in Table 6. Fig. 9 displays the absorption, reflectivity and loss function for ScN and YN. The edge of the optical absorption located at 16.18 nm (25.63 nm) is caused by V_2–C_1 transition between W→Lpoints, which corresponds to the direct band gap X–X: 3.28 eV (W–W: 2.74 eV) for ScN (YN) in HSE hybrid functional. The maximum of absorption is

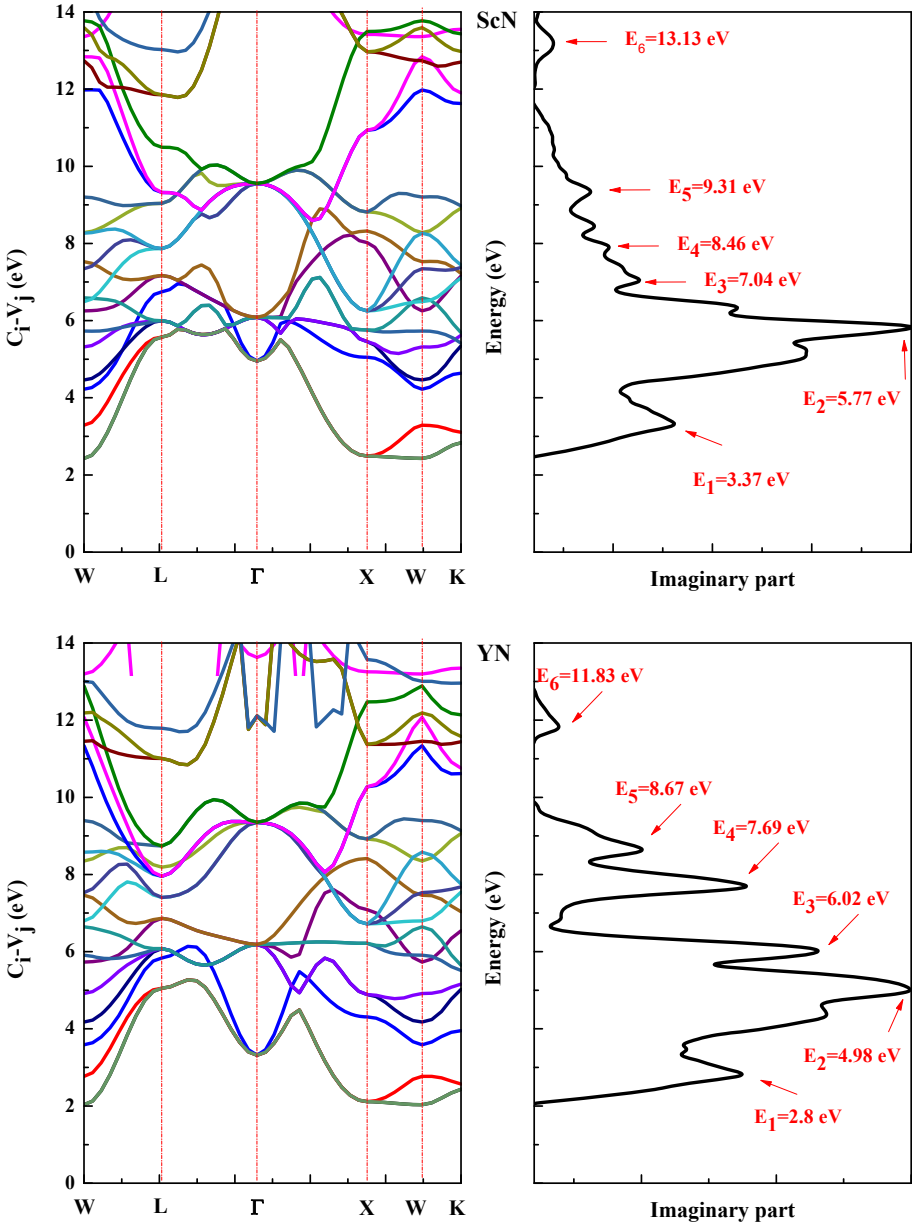

Fig. 8 – Imaginary part (right panel) and transitions energies (left panel). from valence to conduction bands for ScN and YN.

552,709 cm^{-1} (236,303 cm^{-1}) located at 36.9 nm (136.3 nm) for ScN (YN). The maximum reflectivity value is about 0.48 (0.57) at 35.6 nm (121.6 nm) for ScN (YN). ScN and YN show lower reflectivity and consequently higher transmittance. The loss function describes the energy loss when electron traverses a material. Peaks spectrums are associated to plasma resonance with so-called plasma frequency. There are two regions for electronic loss function such as high loss function region located between 28.9 nm and 124 nm (23 nm and 80 nm) for YN (ScN). The second region consists for less than 28.9 nm and beyond 124 nm (23 nm and beyond 80 nm) for YN (ScN). The first region is the high loss region with change of wavelength after the ionization edge. The other is the lower loss function, which can provide information about composition and electronic structure. The amount of light that is incident on the surface of the photo catalytic material that can be estimated from the reflectivity data which is related to the absorbance of that material. After a successive aggrandizement it reached a maximum value of 0.58 (0.48) at 120 nm (35.6 nm) for YN (ScN). The obtained absorption peaks as depicted are attributed to photo transition energies from maximum valence band to minimum conduction band. On can see that maximum of absorption corresponds to the maximum of reflectivity and the no loss function.

Table 6 – The main contribution to the optical spectra originates from all possible transitions between various symmetry points in the Brillouin zone and their corresponding maximum energy.

ScN					
Brillouin zone	W→L	L→Γ	Γ→X	X→W	W→K
E = 3.37eV	$V_2 \rightarrow C_1$				
E = 5.77eV	$V_2 \rightarrow C_2$, $V_3 \rightarrow C_1$ $V_1 \rightarrow C_2$, $V_2 \rightarrow C_3$	$V_1 \rightarrow C_1$, $V_2 \rightarrow C_3$ $V_3 \rightarrow C_1$	$V_2 \rightarrow C_2$, $V_3 \rightarrow C_1$, $V_1 \rightarrow C_2$	$V_2 \rightarrow C_2$ $V_2 \rightarrow C_3$, $V_1 \rightarrow C_3$	$V_2 \rightarrow C_3$ $V_1 \rightarrow C_3$
E = 7.04eV	$V_3 \rightarrow C_3$,$V_3 \rightarrow C_2$	$V_3 \rightarrow C_3$,$V_3 \rightarrow C_1$ $V_3 \rightarrow C_2$	$V_2 \rightarrow C_3$, $V_2 \rightarrow C_5$, $V_3 \rightarrow C_2$	$V_3 \rightarrow C_2$, $V_2 \rightarrow C_5$,$V_2 \rightarrow C_4$	$V_1 \rightarrow C_4$ $V_3 \rightarrow C_2$
E = 8.46eV	$V_3 \rightarrow C_4$	$V_2 \rightarrow C_5$, $V_2 \rightarrow C_4$	$V_2 \rightarrow C_5$ $V_3 \rightarrow C_3$	$V_3 \rightarrow C_4$	$V_3 \rightarrow C_4$
E = 9.31eV	$V_2 \rightarrow C_6$,$V_1 \rightarrow C_6$	$V_2 \rightarrow C_4$, $V_2 \rightarrow C_6$,$V_1 \rightarrow C_4$, $V_2 \rightarrow C_4$	$V_2 \rightarrow C_6$, $V_2 \rightarrow C_5$	$V_3 \rightarrow C_5$	$V_3 \rightarrow C_5$
E = 13.13eV	$V_3 \rightarrow C_6$, $V_2 \rightarrow C_7$ $V_3 \rightarrow C_7$	$V_2 \rightarrow C_7$, $V_3 \rightarrow C_7$	$V_3 \rightarrow C_6$	$V_1 \rightarrow C_7$, $V_2 \rightarrow C_7$	$V_2 \rightarrow C_7$
YN					
Brillouin zone	W→L	L→Γ	Γ→X	X→W	W→K
E = 2.8eV	$V_1 \rightarrow C_1$, $V_2 \rightarrow C_1$		$V_1 \rightarrow C_1$	$V_2 \rightarrow C_1$	
E = 4.98eV	$V_1 \rightarrow C_2$, $V_2 \rightarrow C_2$ $V_2 \rightarrow C_1$, $V_3 \rightarrow C_1$, $V_1 \rightarrow C_1$	$V_1 \rightarrow C_1$, $V_3 \rightarrow C_1$	$V_2 \rightarrow C_2$,$V_3 \rightarrow C_1$, $V_1 \rightarrow C_2$		$V_2 \rightarrow C_2$
E = 6.02eV	$V_3 \rightarrow C_2$, $V_1 \rightarrow C_2$,$V_2 \rightarrow C_2$	$V_3 \rightarrow C_1$, $V_2 \rightarrow C_3$	$V_3 \rightarrow C_2$, $V_2 \rightarrow C_2$	$V_1 \rightarrow C_3$, $V_3 \rightarrow C_2$	$V_3 \rightarrow C_2$ $V_2 \rightarrow C_3$
E = 7.69eV	$V_2 \rightarrow C_4$,$V_1 \rightarrow C_4$	$V_2 \rightarrow C_4$, $V_1 \rightarrow C_4$	$V_2 \rightarrow C_5$, $V_3 \rightarrow C_3$	$V_2 \rightarrow C_5$, $V_3 \rightarrow C_3$	$V_2 \rightarrow C_5$ $V_2 \rightarrow C_4$
E = 8.67eV	$V_3 \rightarrow C_4$, $V_1 \rightarrow C_6$, $V_3 \rightarrow C_5$, $V_3 \rightarrow C_6$	$V_3 \rightarrow C_4$, $V_2 \rightarrow C_6$, $V_2 \rightarrow C_4$, $V_1 \rightarrow C_4$	$V_2 \rightarrow C_4$, $V_3 \rightarrow C_5$	$V_3 \rightarrow C_4$	$V_3 \rightarrow C_4$
E = 11.83eV	$V_3 \rightarrow C_7$, $V_2 \rightarrow C_7$, $V_3 \rightarrow C_6$, $V_2 \rightarrow C_6$	$V_3 \rightarrow C_7$, $V_2 \rightarrow C_7$, $V_1 \rightarrow C_7$	$V_3 \rightarrow C_6$, $V_2 \rightarrow C_7$	$V_2 \rightarrow C_7$, $V_2 \rightarrow C_6$	$V_2 \rightarrow C_7$, $V_3 \rightarrow C_6$

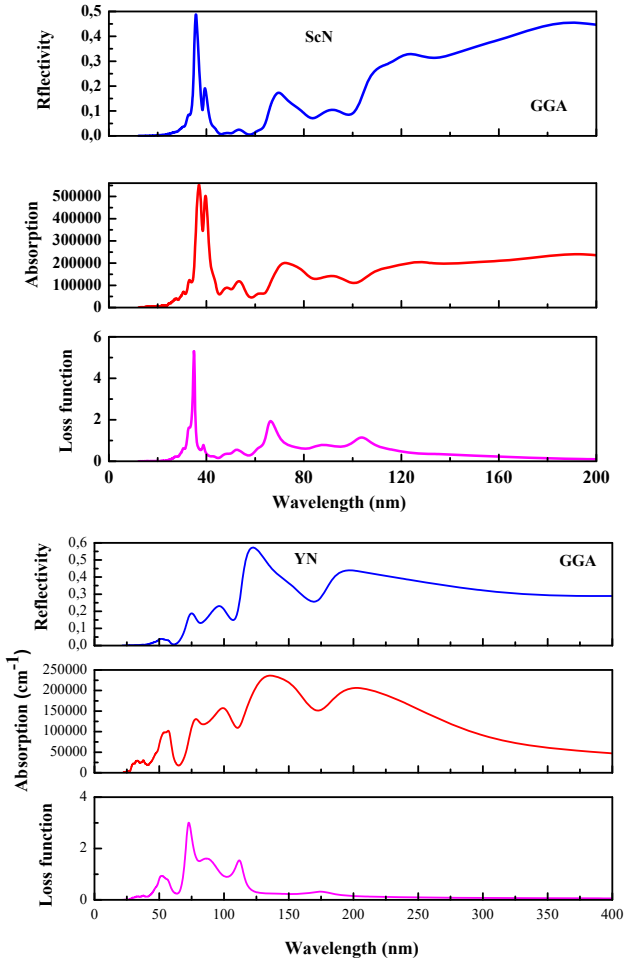

Fig. 9 – Reflectivity, absorption and loss function versus wave length for ScN and YN in the zinc blend structure.

4. Conclusion

We have carried out studies on scandium and yttrium nitrides semiconducting in the zinc blend structure by ab-initio method. The lattice constant, the bulk modulus and its pressure derivative are analyzed and compared with experimental and other theoretical data. The absence of experimental and theoretical elastic constants, band gaps and transitions between various symmetry points in the Brillouin zone of scandium and yttrium nitrides in the zinc blend structure make our results as predictions. The shear modulus, Young's modulus, Poisson's ratio are estimated using Voigt–Reuss–-Hill approximations for scandium and yttrium nitrides in the zinc blend structure. The bands profile indicates that ScN (YN) has a direct X–X (W–W) band gap of 2.4 eV, 2.28 eV, 2.34 eV and 3.28 eV (2.01 eV, 2.10 eV, 2.14 eV and 2.74 eV) for GGA, LDA, GGA-PBESOL and HSE hybrid functional. The hybridization between Sc: d (Y: d) and N: p sites at the upper valence band translates the covalent bonding character for N–Sc and N–Y. The optical transition occurs from Sc: d (Y: d) or N: p states to Sc: p (Y: p) site. The maximum of longitudinal (acoustical) branches is located between L and Γ (at L and X) points. The optical absorption edge located at 16.1 nm (25.6 nm) is caused by V_2–C_1 transition between W→L and corresponds to the direct band gap X–X: 3.28 eV (W–W: 2.74 eV) for ScN (YN) in HSE hybrid functional. Scandium and yttrium nitride interest the researchers as absorbent materials, due to their high optical absorption, low reflectivity, low cost, tunable band gap and high conversion efficiency for photovoltaic applications. N: p orbit and small contribution of Sc: d (Y: d) site are responsible to optical modes, while Sc: d (Y: d) orbit and few participation of N: p site contribute to acoustical modes. The electronic contribution at the top of the valence band is

provided by N: p site and Y: d (Sc: d) orbit, with small participation of Y: s and Y: p (Sc: s and Sc: p) sites for YN (ScN).

Declaration of Competing Interest

The authors declare that they have no known competing financial interests or personal relationships that could have appeared to influence the work reported in this paper.

Acknowledgements

The authors acknowledge Taif University Research Supporting Project number (TURSP-2020/66), Taif University, Taif, Saudi Arabia.

REFERENCES

[1] Bidai K, Ameri M, Ameri I, Bensaid D, Slimani A, Zaoui A, et al. Arch Metall Mater 2017;62:865–71.
[2] Gall D, Petrov I, Hellgren N, Hulman L, Sundgren J-E, Greene JE. J Appl Phys 1998;84:6034.
[3] Bai X, Kordesch ME. Appl Surf Sci 2001;175–176:499.
[4] Eklund Per, Sit Kerdsongpanya, Alling Björn. J Mater Chem C 2016;4:3905–14.
[5] Liu Jian, Li Xi-Bo, Zhang Hui, Yin Wen-Jin, Zhang Hai-Bin, Peng Ping, et al. J Appl Phys 2014;115(9):093504.
[6] Qteish A. Phys Rev B 2006;74:245208.
[7] Xue Wenhui, You Yu, Zhao Yuna, HuiLei Han, Tao Gao. Comput Math Sci 2009;45:1025.
[8] Gall D, Stadele M, Jarrendahl K, Petrov I, Desjardins P, Haasch RT, et al. Phys Rev B 2001;63:125119.
[9] Takeuchi N. Phys Rev B 2002;65:045204.
[10] Stampfl C, Mannstadt W, Asahi R, Freeman AJ. Phys Rev B 2001;63:155106.
[11] Cruz WDL, Duaz JA, Mancera L, Takeuchi N, Soto G. J Phys Chem Solid 2003;64:2273.
[12] Lü T-Y, Huang M-C. Chin Phys 2007;16(1):62.
[13] Biswas B, Saha B. Phys. Rev. Mater. 2019;3(2):020301.
[14] Ul Haq Bakhtiar, Afaq A, Abdellatif Galila, Ahmed R, Naseem S, Khenata R. Superlattice Microst 2015;85:24–33.
[15] More-Chevalier Joris, Cichoň Stanislav, Bulíř Jiří, Poupon Morgane, Hubík Pavel, Fekete Ladislav, et al. AIP Adv 2019;9(1):015317.
[16] Liu Jian, Li Xi-Bo, Zhang Hui, Yin Wen-Jin, Zhang Hai-Bin, Peng P, et al. J Appl Phys 2014;115(9):093504. https://doi.org/10.1063/1.4867515.
[17] Jena Debdeep, Ryan Page, Joseph Casamento, Dang Phillip, Singhal Jashan, Zhang Zexuan, et al. Jpn J Appl Phys 2019;58:0801. Number SC.
[18] Segall MD, Lindan PJD, Probert MJ, Pickard CJ, Hasnip PJ, Clark SJ, et al. J Phys Condens Matter 2002;14:2717.
[19] Vanderbilt D. Phys Rev B 1990;41:7892.
[20] Goedecker S, Teter M, Hutter J. Phys Rev B 1996;54:1703.
[21] Perdew JP, Burke K, Ernzerhof M. Phys Rev Lett 1996;77:3865.
[22] Semari F, Dahmane F, Baki N, Al-Douri Y, Akbudak S, Uùgur G, et al. Chin J Phys 2018;56:567–73. https://doi.org/10.1016/j.cjph.2018.01.015.
[23] Monkhorst HJ, Pack JD. Phys Rev B 1976;13:5188.
[24] Fischer TH, Almlof J. J Phys Chem 1992;96:9768.
[25] Benkaddour Y, Abdelaoui A, Yakoubi A, Khachai H, Al-Douri Y, Bin Omran S, et al. J Superconduct Novel Magnet 2018;31:395–403.
[26] Feng W, Cui S, Hu H, Zhang G, Lv Z, Gong Z. Physica B 2010;405:2599.
[27] Kaurav N, Kuo YK, Joshi G, Choudhary KK, Varshney Dinesh. High Pres Res 2008;28(4):651–63.
[28] Takeuchi N. Phys Rev B 2002;65. 045204-1.
[29] Berkok Houria, Tebboune Abdelghani, Saim Asmaa, Belbachir Ahmed H. Physica B 2013;411:1–6.
[30] Yagoub R, Hadjfatah A, Louhibi-Fasla S, Daoud S, Bahlouli S, Haichour A, et al. J Nano-Electron Phy 2020;12(5). 05009-05014.
[31] Shirotani I, Yamanashi K, Hayashi J, Ishimatsu N, Shimomura O, Kikegawa T. Solid State Commun 2003;127:573.
[32] Pettifor DG. Mater Sci Technol 1992;8:345.
[33] Boudiaf K, Bouhemadou A, Al-Douri Y, Khenata R, Bin-Omran S, Guechi N. J Alloys Compd 2018;759:32–43.
[34] Shoaib M, Murtaza G, Khenata R, Farooq M, Ali Roshan. Comput Mater Sci 2013;79:239–46.
[35] Bhardwaj P, Singh S, Gaur NK. Mater Res Bull 2009;44:1366.
[36] Amal Mentefa, Fatima Zohra Boufadi, Mohammed Ameri, Feriel Ouarda Gaid, Loubna Bellagoun, Ali Abu Odeh. J Superconduct Novel Magnet 2021;34:269–83.
[37] Fadila Belkharroubi, Ameri Mohammed, Bensaid Djillali, Noureddine Moulay, Ameri Ibrahim, Mesbah Smain, et al. J Magn Magn Mater 2018;448:208–20.
[38] Mohammed Ameri, Faiza Bennar, Slamani Amel, Ameri Ibrahim, Al-Douri Y, Dinesh Varshney. Phase Transit 2016;89:1236–52.
[39] Nye JF. Physical properties of crystals. Oxford): Oxford University Press; 1985.
[40] Ameri M, Slamani A, Abidri B, Ameri I, Al-Douri Y, Bouhafs B, et al. Mater Sci Semicond Proc 2014;27:368–79.
[41] Moussali A, Amina MB, Fassi B, Ameri I, Ameri M, Al Douri Y. Indian J Phys 2020;94:1733–47.
[42] Touam S, Belghit R, Mahdjoubi R, Meghdoud Y, Meradji H, Khan Muhammad Shehryar, et al. Bull Mater Sci 2020;43:22. https://doi.org/10.1007/s12034-019-1978-y.
[43] Guechi N, Bouhemadou A, Medkour Y, Al-Douri Y, Khenata R, Bin Omran S. Phil Mag 2020;100:3023–39.
[44] Voigt W. Lehrbuch der Kristallphysik. Leipzig: Teubner Verlag; 1928.
[45] Reuss A, Angew Z. Math Mech. 1929;9:49–58.
[46] Hill R. Proc Phys Soc London A 1952;65:349.
[47] Kada Bidai, Mohammed Ameri, Zaoui Ali, Ibrahim Ameri, Yarub Al-Douri. Chin J Phys 2016;54:678–94.
[48] Ayad M, Belkharroubi F, Boufadi FZ, Khorsi M, Zoubir MK, Ameri M, et al. Indian J Phys 2020;94:767–77.
[49] Bidai Kada, Ameri Mohammed, Amel Slamani, Ameri Ibrahim, Al-Douri Y, Varshney Dinesh, et al. Chin J Phys 2017;55:2144–55.
[50] Mattesini M, Magnuson M, Tasnádi F, Höglund C, Abrikosov Igor A, Hultman L. Phys Rev B 2009;79:125122.
[51] Yahiaoui IE, Lazreg A, Dridi Z, Al-Douri Y, Bouhafs B. Bull Mater Sci 2018;41. https://doi.org/10.1007/s12034-017-1516-8. 2.
[52] Benkabou MH, Harmel M, Haddou A, Yakoubi A, Baki N, Ahmed R, et al. Chin J Phys 2018;56:131–44.
[53] Bekhti-Siad A, Bettine K, Rai DP, Al-Douri Y, Wang Xiaotian, Khenata R, et al. Chin J Phys 2018;56:870–9.
[54] Leila Hasni, Mohammed Ameri, Djillali Bensaid, Ameri Ibrahim, Smain Mesbah, Yarub Al-Douri, et al. J Superconduct Novel Magnet 2017;30:3471–9.
[55] Hadji S, Bouhemadou A, Haddadi K, Cherrad D, Khenata R, Bin-Omran S, et al. Physica B 2020;589:412213.